



OTC 4490

Drag Coefficients of Long Flexible Cylinders

by J. Kim Vandiver, *Massachusetts Inst. of Technology*

Copyright 1983 Offshore Technology Conference

This paper was presented at the 15th Annual OTC in Houston, Texas, May 2-5, 1983. The material is subject to correction by the author. Permission to copy is restricted to an abstract of not more than 300 words.

ABSTRACT

In the summer of 1981 a field experiment was conducted investigating the vibration response of long flexible cylinders to vortex shedding in a steady, uniform current. Two basic cylinder types were tested, both 75 feet in length. One cylinder was a cable 1.25 inches in diameter with seven pairs of internal biaxial accelerometers. The second cylinder was a steel pipe, 1.631 inches in diameter, carrying the cable inside. Drag force, current speed, tension, and biaxial acceleration at seven locations were measured. Drag coefficients in excess of 3.0 were measured for both the pipe and the cable under lockin conditions.

INTRODUCTION

Flow induced vibration problems have been confronting engineers for many years. Recent problems encountered at deepwater sites with substantial currents have generated a renewed concern for vortex induced vibration problems. Drilling risers, TLP tension members, suspended pipeline spans, and mooring cables are all subject to vibration related failure.

Considerable experimental work has been conducted on short cylindrical segments under controlled laboratory conditions. Mean drag coefficients as high as 3.0 have been demonstrated with cross flow lockin of spring mounted or driven rigid cylinders. There has been an understandable reluctance on the part of designers to use such high values in design. In fact many engineers find it hard to believe that such high drag coefficients are possible under realistic field conditions with long flexible cylinders.

The purpose of the experiment described in this paper was to measure the flow-induced vibration response of a long flexible

cylinder under more realistic, but still uncontrolled, field conditions. These tests were more realistic than laboratory ones, because it was possible to use a cylinder of sufficient length that many different natural modes could be excited. At the same time, reasonably high Reynolds numbers could be achieved.

These tests were controlled in that the flow velocity was uniform over the length of the cylinder, and tension, current and vibration could be easily measured. With substantial effort drag measurements were also made, a task which is at times a challenge even under laboratory conditions.

THE TEST SITE AND INSTRUMENTATION

The Test Site

The site chosen for the experiment was a sandbar located at the mouth of Holbrook Cove near Castine, Maine. This was the same site used for previous experiments during the mid-1970's by Vandiver and Mazel (1,2). At low tide the sandbar was exposed allowing easy access to the test equipment, while at high tide it was covered by about ten feet of water. The test section was oriented normal to the direction of the current which varied from 0 to 2.4 ft/s over the tidal cycle with only small spatial variation over the test section length at any given moment.

The data acquisition station for the experiment was the R/V Edgerton which was chartered from the MIT Sea Grant Program. The Edgerton was moored for the duration of the experiment approximately 300 feet from the sandbar and connected to the instruments on the sandbar by umbilicals.

Prior to the data acquisition phase of the experiment, several days were needed to prepare the site. A foundation for the experiment was needed to anchor the supports which were to hold the ends of the test cylinders. To accomplish this, six 4.5 inch

References and illustrations at end of paper.

diameter steel pipes were water jetted into the sandbar utilizing the fire pump aboard the Edgerton. These six pipes were made of two five foot sections joined by couplings so that the overall length of each was ten feet. In addition, one two-inch diameter by six foot long steel pipe was jetted into the sandbar to be used as a current meter mount. Finally, a section of angle iron was clamped to the pipe used to support the drag measuring mechanism and attached to another support pipe to prevent any rotation of the drag mechanism mount. Figure 1 shows a schematic diagram of the set-up of the experiment.

Test Instrumentation

Drag measurement system. The drag measurement system was located at the west end of the cable system as shown in Figure 1. The device was welded onto a support pipe 2.5 feet above the mudline. The mean drag force at the termination of the cable was used to generate a moment about a freely rotating vertical shaft located a few inches beyond the termination point. The bearings supporting the shaft carried the entire tension load without preventing rotation. The moment was balanced by a load cell which restrained a lever arm connected to the shaft (see Figure 2). From the known lever-arm lengths and the load cell measurements the mean drag force on one half of the cable could be determined. The load cell signal was carried by wires in the cable and umbilical to the Edgerton where it was conditioned and recorded.

Current measurement system. The current was measured by a Neil Brown Instrument Systems DRCM-2 Acoustic Current Meter located 12.5 feet from the west end of the test cable and 2 feet upstream. It was set so that it determined both normal and tangential components of the current at the level of the test cable. Signals from the current meter traveled through umbilicals to the Edgerton where they were monitored and recorded. In addition, a current meter traverse was made using an Endeco current meter to determine any spatial variations in current along the test section. The current was found to be spatially uniform to within 3.0 percent from end to end for all but the lowest current speeds ($V < 0.5$ ft/s)

Tension measurement system. The tension measuring and adjusting system was located at the east end of the experimental test set up (see Figure 1). Extensions were made to two of the posts at this end. As shown in the diagram, a five foot extension was made to the center post and a three foot extension was made to the innermost post. This three foot extension was hinged at the mudline. Onto this pivoting post, a hydraulic cylinder was mounted 2.5 feet above the mudline. The test cable in the experiments was connected to this hydraulic cylinder. To the back of the hydraulic cylinder one end of a Sensotec Model RM In-Line load cell was connected.

The other end of the cell was attached via a cable to the anchor posts. The output from the tension load cell was transmitted through the umbilicals to the Edgerton where it was monitored. Hydraulic hose ran from a hand operated pump on the Edgerton to the hydraulic cylinder so that the tension could be changed as desired. Additional details concerning the test instrumentation are given by McGlothlin (3).

The Test Cable

A 75 foot long composite cable was developed specifically for the experiments that were conducted in the summer of 1981. Figure 3 shows a cross-section of the test cable. The outer sheath for this cable was a 75 foot long piece of clear flexible PVC tubing, which was 1.25 inches in outside diameter and 1.0 inch inside diameter. Three 0.125 inch stainless steel cables ran through the tubing and served as the tension carrying members. A cylindrical piece of 0.5 inch O.D. neoprene rubber was used to keep the stainless steel cables spaced 120 degrees apart. The neoprene rubber spacer was continuous along the length except at seven positions where biaxial pairs of accelerometers were placed. Starting at the east end, these positions were at $L/8$, $L/6$, $L/4$, $2L/5$, $L/2$, $5L/8$, and $3L/4$. These accelerometers were used to measure the response of the cable as it was excited by the vortex shedding. The accelerometers were Sundstrand Mini-Pal Model 2180 Servo Accelerometers which were sensitive to the direction of gravity. The biaxial pairing of these accelerometers made it possible to determine their orientation and to extract cross flow and in-line accelerations of the cable at the seven locations.

Three bundles of ten wires each ran along the sides of the neoprene spacer to provide power and signal connections to the accelerometers and also to provide power and signal connections to the drag measuring system. Finally, an Emerson and Cuming flexible epoxy was used to fill the voids in the cable and make it watertight. The weight per unit length of this composite cable was 0.77 lb/ft in air.

The Test Pipe

For some tests the instrumented cable was placed inside a steel tube with a 1.631 inch outside diameter and a 1.493 inch inside diameter. The tube made was made up of four equal length sections joined together by threaded couplings. The ends of the tubing were connected to the drag cell and the hydraulic ram by custom-made universal joints. These special terminations applied the primary tension to the pipe, but also applied a small tension to the internal cable. Neoprene spacers placed at eighteen inch intervals prevented any relative motion between the cable and the tube. The remaining cavity was allowed to fill with water. The weight per unit length of the steel tubing with the cable inside and the

voids filled with water was 2.234 lbs/ft. The bending stiffness, EI, was measured at $3.11 \times 10^6 + 0.05 \times 10^6$ lb-in².

The mechanical properties of the cable and the pipe are summarized in Table I.

Data Acquisition Systems

During the experiment, data taken from the instruments on the sandbar were recorded in two ways. First, analog signals from the fourteen accelerometers in the cable as well as current and drag were digitized, at 30.0 Hz per channel, onto floppy disks using a Digital Equipment MINC-23 Computer. Second, analog signals from the drag cell, current meter, and six accelerometers were recorded by a Hewlett-Packard 3968A Recorder onto eight-track tape. The disks were limited to record lengths of eight and one half minutes and were used to take data several times during each two and one half hour data acquisition period. A Hewlett-Packard 3582A Spectrum Analyzer was set up to monitor the real time outputs of the accelerometers. The eight-track tape was used to provide a continuous record of the complete two and one half hour data cycle.

The Attached Masses

In some experiments, lumped masses were fastened to the bare cable to simulate the effects of hydrophones and oceanographic instruments. The lumped masses were made of cylindrical PVC stock and each was 12.0 inches long and 3.5 inches in diameter. A 1.25 inch hole was drilled through the center of each lumped mass so that the cable could pass through. In addition, four 0.625 inch holes were drilled symmetrically around his 1.25 inch center hole so that copper tubes filled with lead could be inserted to change the mass of the lumps. In the field, it was difficult to force the cable through the holes drilled in the PVC so the masses were split in half along the length of their axes. The masses were then placed on the cable in halves and held together by hose clamps. Different tests were run by varying the number and location of lumped masses and by changing the mass of the attachments. The weight of a lump in air with no lead was 4.41 pounds, and with lead was 9.97 pounds.

The Strumming Suppression Fairing

In one test a stranded strumming suppression device was attached to the test cable. The material was 11 1/2 inches long by 1/16 inch diameter strands of a very flexible plastic. The strands were densely attached to the cable by a braid of stainless steel wire. This suppression device is commercially available from Endeco, and was donated for testing. The appearance of the cable is that of a cylinder with long strands of closely spaced thick plastic hair.

THE MEASUREMENT PROGRAM

In Air Tests

The cable, the cable with lumps, and the pipe were all tested in air at low tide. The purpose of these tests was to obtain measured damping values for the first few natural modes of vibration, and to allow comparisons between measured and predicted values of natural frequencies.

It was possible to resonantly excite modes 2, 3 or 4 by simply driving the cable by hand near an anti-node. Transient decay values yielded estimates of the damping.

For the cable at a typical tension of 792 pounds the damping was between 0.2 and 0.5% of critical. For the pipe at a tension of 1,000 pounds typical values of damping for modes 2, 3, and 4 were 0.1 to 0.5%. The cable with lumped masses had similar values of damping. The natural frequencies of the cable and the pipe under tension are given by:

$$\text{Cable: } \omega_n = \frac{n\pi}{L} \sqrt{T/m}$$

$$\text{pipe: } \omega_n = \left[\frac{T}{m} \left(\frac{n\pi}{L} \right)^2 + \frac{EI}{m} \left(\frac{n\pi}{L} \right)^4 \right]^{1/2}$$

where L = length, 75 feet

T = tension, lbs

m = mass/ft, slugs

EI = bending rigidity, lb-ft²

n = mode number.

The mode shapes for both the cable, and the pipe under tension with pinned ends are sinusoids given by:

$$Y_n(x) = \sin \left(\frac{n\pi x}{L} \right)$$

The predicted and measured natural frequencies in air were within 1% of one another. The natural frequencies and mode shapes of the cable with lumps were predicted using a program called NATFREQ, which was developed for the Naval Civil Engineering Laboratory by Bill Iwan at Cal Tech. A complete description of the comparison for the cable with various lump configurations is discussed in Reference 4.

In Water Tests

On each rising tide it was possible to acquire useful data for 2.5 hours, terminating at high water. During these periods, simultaneous measurements of current, tension, acceleration and drag force were made. Typically, one test was made per day. Several days were devoted to each: the cable, the pipe, and the cable with various lumped mass configurations. The entire field

program spanned nearly six weeks. In this paper, a macro view of the drag coefficient data is emphasized. In later papers, a detailed normal mode analysis of the vibration and a correlation of individual vibration modes to observed drag coefficient data is anticipated.

During the tests the current speed varied from 0 to 2.4 feet/second. The seawater temperature was 12 to 14 degrees Celsius. The maximum Reynolds number achieved for the pipe was approximately 22,000.

A MACRO VIEW OF THE DRAG COEFFICIENT DATA

Figure 4 presents a summary of the drag coefficient, current, and RMS displacement response for the steel pipe for one entire 2 1/2 hour data acquisition cycle. The drag coefficient was computed using the following equation.

$$C_D = \text{Total Mean Drag Force} / (1/2 \rho D L V^2)$$

where ρ , D , L , and V are the water density, cylinder diameter and length, and current speed, respectively. The drag force transducer measured only the drag at one end of the cylinder. Symmetry was assumed and the measured value was doubled to obtain the total drag force. All values presented were computed using an 8.55 second moving average. As presented the current speed is in units of feet/second, and the RMS displacements are in inches. The RMS displacements are those measured at one sixth of the pipe's total length in from the east end. These displacements were obtained by double integration of the accelerometer signals in both the cross flow (vertical) and in-line (horizontal) directions. These displacements have not been corrected for mode shape. The position $L/6$ may be near an antinode for some modes and near a node for others. By normal mode analysis the individual modal contributions may be extracted, but those results are not reported on here.

In this example, the drag coefficients vary from 1.6 to 2.8, compared to the expected rigid cylinder value of 1.2. The high spike on the left resulted from an encounter with a large piece of seaweed and should be disregarded. An important feature is the occurrence of the occasional high plateaus in drag coefficient. These plateaus correspond to periods of lockin. At these times, the vortex shedding process synchronized with a natural frequency of the pipe in the cross-flow direction. For the current speeds and tensions (670-920 lbs) in this example, lockin frequently involved the second or third modes of vibration. Two such plateaus are noted on the figure.

Under conditions of lockin, the cross-flow response was harmonic at a single frequency, with antinode displacements of \pm one diameter. The in-line vibration was usually dominated by vibration at twice the cross-flow frequency because the unsteady

drag forces occur at twice the vortex shedding frequency.

Under lockin conditions the RMS response in both the cross-flow and in-line directions also increases to a steady plateau value in the figure. With sufficient change in flow velocity the lockin process is disrupted and the RMS response and drag coefficient decrease. The cross-flow vortex induced excitation decreases in spatial correlation length and increases in frequency bandwidth, becoming a band limited random excitation. Several modes typically respond simultaneously under these conditions. Many examples of these periods of non-lockin can be seen between the high plateaus in drag coefficient and displacement.

The error bounds on the current measurements are approximately $\pm .05$ feet/second. The total error on the C_D values including the effects of the current and force measurement are about $\pm 15\%$ at 1.0 foot/second decreasing to $\pm 10\%$ at 2.0 feet/second. At current speeds below 1.0 foot/second the C_D values become less reliable.

Similar plots are presented for tests of the bare cable, the cable with the fairing and the cable with six lumped masses. The bare cable response is distinguished by very high values of C_D , typically from 2.5 to 3.5, and by the lack of obvious lockin plateaus. The tension for this test varied from 320 lbs to 600 lbs, and the modes for which lockin was possible included the second to the sixth. Upon inspection of time history data, lockin response is frequently observed. Because the total forces measured on the cable are smaller, the drag coefficient calculations are not as accurate as for the pipe, and are accurate to approximately $\pm 15\%$ from 1.0 to 2.0 feet per second.

The record for the cable with the long stranded suppression material is distinguished by three features. The drag coefficients are lower, ranging from 2.0 to 2.8. Very pronounced lockin plateaus occur in the RMS data, likely corresponding to the third mode of vibration. The drag coefficient and RMS displacement plots are much smoother, indicating much less rapid temporal variation in the response. This suggests that the strands were effective in damping out the high frequency overtones which are commonly present in the response. The material succeeds in reducing the drag coefficient somewhat by decreasing the total amplitude of vibration, even though the large surface area of the strands probably adds, but to a lesser extent, to the total drag of the system. The tension range for this example was from 500 to 800 pounds.

It should be noted that the highest tensions in all tests correspond to the highest flow speeds. This was because the hydraulic ram, fixed the straight line distance between the connection points. As

drag forces increased with current, the tension increased also.

The distinguishing feature of the data for the cable with lumps is that again very prominent lockin plateaus become evident. The drag coefficients vary from 2.2 to 3.0. The tension range was 500 to 800 pounds and the likely responding cross-flow modes were from second to the fifth. The lumps were located at: Light lumps at L/8 and L/2, heavy lumps at L/3, 5L/8, 3L/4, and 7L/8.

A DISCUSSION OF VIBRATION RESPONSE

It has been suggested that the vibration response may be divided into two categories: lockin and non-lockin. For the Castine tests lockin behavior corresponded to the synchronous shedding of vortices with the resonant vibration of a single natural mode in the cross-flow direction. This coherent excitation of the entire length of the cylinder is characterized by harmonic response at the natural frequency of the mode. At the same time, drag force fluctuations at twice the frequency of the lift force fluctuations causes a coherent in-line response typically terminated by one mode also.

Figure 8 is an example two dimensional trace of the motion of the pipe at its midpoint, L/2, under lockin conditions. In this particular case the cross flow motion was in the third vibration mode. The natural frequency of the fifth mode in the in-line direction was exactly twice the third cross-flow natural frequency. Therefore the in-line fifth mode response was resonant with the drag force fluctuations. The center of the pipe is an antinode for both the third and the fifth mode. The phasing of the lift and drag forces in this case was such that figure eight motion results. The cross-flow vibration amplitude is one diameter and the in-line is one-half a diameter.

Under non-lockin conditions the spatial coherence of the vortex shedding process is greatly reduced, and the bandwidth of the local lift and drag forces increases from a single frequency at lockin to a band limited random process. The bandwidth of the excitation sometimes includes several natural frequencies of the cable. The drag force spectrum has significant levels at frequencies twice that occurring in the lift force spectrum.

A typical two dimensional trace of the motion of the pipe at L/8 is shown in Figure 9. On the average, the cross-flow response substantially exceeds the in-line response. The RMS amplitude is less than that seen at lockin. However, occasional peaks occur which may exceed the peak amplitudes under lockin conditions. For the example shown in Figure 9 the cross-flow motion was a superposition of modes 2, 3, 4 and 5, and the in-line vibration included the response of modes 4, 5, 6, and 7.

Over the years a great deal of emphasis has been placed on the study of lockin phenomena. For long cables, and risers in actual non-uniform flow conditions, non-lockin response may be of greater concern, especially under circumstances in which fatigue is a problem. Though infrequent, peak stresses under non-lockin conditions may exceed those occurring under lockin conditions.

THE RELATIONSHIP BETWEEN VIBRATION AMPLITUDE AND DRAG COEFFICIENT

Vibration response amplitude and drag coefficient are known to be closely coupled. The Castine data provides absolute verification that this is also true under field conditions. Figure 10 is an excellent example of this. This is a record of RMS displacement, drag coefficient, and current over a 490 second time period. Over this period the response of the pipe was dominated by lockin in the third mode, as in Figure 8. The moving average window for the figure was shortened to 2.33 seconds to reveal short term variations. Note the nearly exact coincidence between short term fluctuations in cross-flow displacement and drag coefficient. A similar dependence of drag coefficient on RMS response has been observed during periods of non-lockin cylinder vibration.

THE PREDICTION OF DRAG COEFFICIENTS

Skop, Griffin, and Ramberg proposed an empirical relation for the prediction of drag coefficients under lockin conditions (5). This equation was modified slightly for use with our data, and is given below.

$$C_D = C_{DO} \left[1 + 1.043 (2Y_{RMS}/D)^{0.65} \right]$$

where Y_{RMS}/D is the root mean square antinode displacement in diameters. C_{DO} is the rigid cylinder value of drag coefficient appropriate for the test cylinder; which for the Castine tests is 1.2.

This equation was used to predict drag coefficient for cases of lockin with the cable and the pipe. The results were very good. The predicted and measured values for the pipe were virtually indistinguishable. The predicted values for the cable were about 15% lower than observed. This is within the expected error bounds on the measured values for the cable.

CONCLUSIONS

The goal of this experiment was to extend the knowledge of flow induced vibration gathered under very constrained laboratory conditions to that obtained under controlled but less constrained field conditions. Tests were successfully conducted on cylinders with length to diameter ratios of approximately 750 and at Reynolds numbers up to 22,000. For the first

time drag coefficients were obtained on flexible cylinders exhibiting substantial vibration in up to the seventh mode.

Under uniform flow lockin conditions drag coefficients in excess of three were measured. These are shown to be in agreement with drag coefficients predicted using an empirical formula based largely on laboratory data.

It is not the intention of the author to suggest that drag coefficients of three must be used in design of deep water flexible cylinders. There are many reasons that this may not be appropriate. Such high drag coefficients were only observed under spatially uniform flow conditions and lockin vibration. Under non-lockin random vibration response conditions the amplitude of vibration and drag was substantially reduced.

Under actual field conditions the flow is usually not spatially uniform, leading to different vortex shedding frequencies at different locations. Vibration response is likely to be more broadband in frequency content and lower in RMS amplitude than that of a lockin. Mean drag coefficients will likely be less as well.

Vibration response under non-lockin conditions is reasonably well described as a Gaussian random process. Because of this there are frequent occasions that response peaks occur, well in excess of those observed at lockin. For this reason non-lockin vibration may be more of a fatigue threat, because it gives rise to larger stress range cycles.

Close examination of non-lockin data from Castine reveals that the mean drag force increases and drags over time periods of many seconds. This suggests that very long period natural modes might be excited at frequencies far lower than vortex shedding frequencies.

The most important topic in this field needing research attention is the vibration response of long cylinders in spatially non-uniform or shear flows. An excellent opportunity would be the monitoring of the vibration of drill pipe suspended beneath an exploration drill ship in deep water on the Atlantic Coast.

There is at present a joint industry sponsored project at MIT, focussing on the random vibration analysis of the non-lockin data from the Castine experiment and also on the analysis of flow induced vibration in shear flows. The shear flow research will include field experiments.

ACKNOWLEDGEMENTS

This research was part of a joint industry and government sponsored project supported by the American Bureau of Shipping, Brown and Root, Inc., Chevron Oil Field Research, Conoco, Inc., Exxon Production

Research, Shell Development Company, Union Oil Research, the Office of Naval Research, and the U.S. Geological Survey.

An eight member team led by Professor J. Kim Vandiver participated in the field experiments. Prof. Vandiver was assisted during these experiments by Charles Mazel, Jen-Yi Jong, Ed Moas, Peter Stein, Mark Whitney, Pam Vandiver, and Jim McGlothlin. Most of the data processing for the results presented in this paper was done by Jim McGlothlin (3) and Jen-Yi Jong.

REFERENCES

1. J.K. Vandiver and C.H. Mazel, "A Field Study of Vortex-Excited Excited Vibrations of Marine Cables," Offshore Technology Conference Paper OTC24291 (May 1976).
2. J.K. Vandiver and T.W. Pham, "Performance Evaluation of Various Strumming Suppression Devices," MIT Ocean Engineering Department Report 77-2 (March 1977).
3. J.C. McGlothlin, "Drag Coefficients of Long Flexible Cylinders Subject to Vortex Induced Vibrations," M.S. Thesis, MIT Ocean Engineering Department (January 1982).
4. J.K. Vandiver and O.M. Griffin, "Measurements of the Vortex Excited Strumming Vibrations of Marine Cables," Proceedings Ocean Structural Dynamics Symposium '82, Corvallis, Oregon, (September 1982).
5. R.A. Skop, O.M. Griffin, and S.E. Ramberg, "Strumming Predictions for the SEACON II Experimental Mooring," Offshore Technology Conference Preprint OTC 2491 (May 1977).

TABLE I

MECHANICAL PROPERTIES AND DIMENSIONS
OF TEST CYLINDERS

Cable Specifications:

Length:	75.0 \pm .1 feet
Diameter:	1.25 \pm 0.02 inches
Weight per foot in air:	0.7704 pounds per foot
Mass per foot:	0.0239 slugs per foot in air
Specific gravity:	1.408

Pipe Specifications:

Length:	75.0 \pm 0.02 feet
Outside Diameter:	1.631 \pm .003 inches
Inside Diameter:	1.493 \pm .003 inches
Weight per foot in air:	1.231 pounds per foot
Weight per foot in air including weight of the internal cable:	2.001 pounds per foot
Weight per foot including cable and trapped water:	2.236 pounds per foot
Specific gravity of pipe with cable and trapped water:	2.40
Measured bending stiffness, EI:	(3.106 \pm .05) $\times 10^6$ pound inches. ²

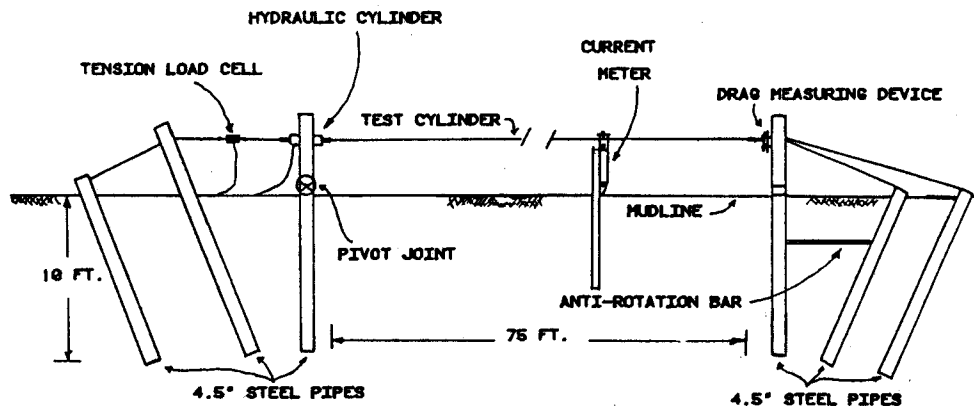


Fig. 1—Schematic diagram of the experiment.

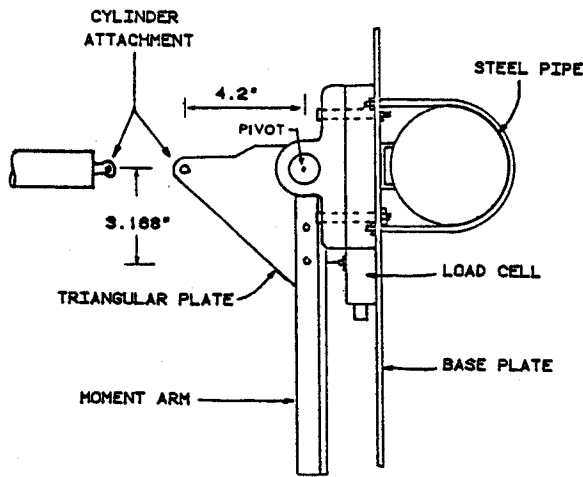


Fig. 2—Top view of the drag measuring device.

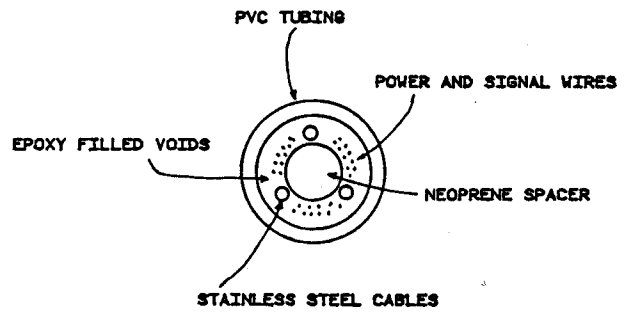


Fig. 3—Section of the test cable.

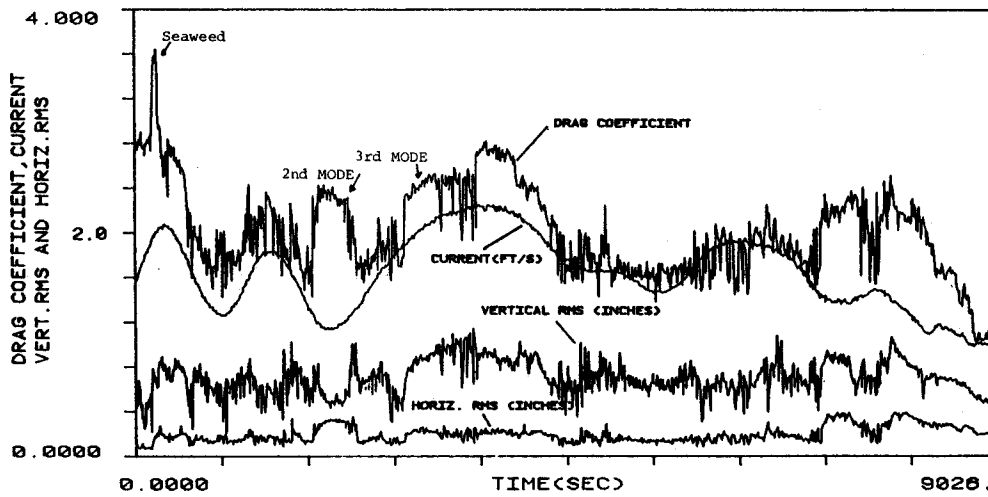


Fig. 4—Drag coefficient, current, and RMS displacement at L/6 for the pipe.

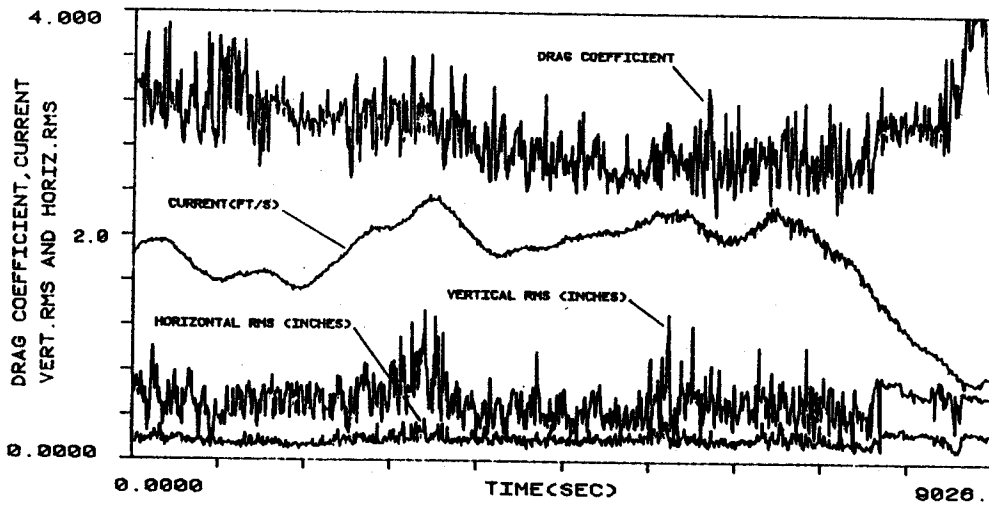


Fig. 5—Drag coefficient, current, and RMS displacement at L/6 for the bare cable.

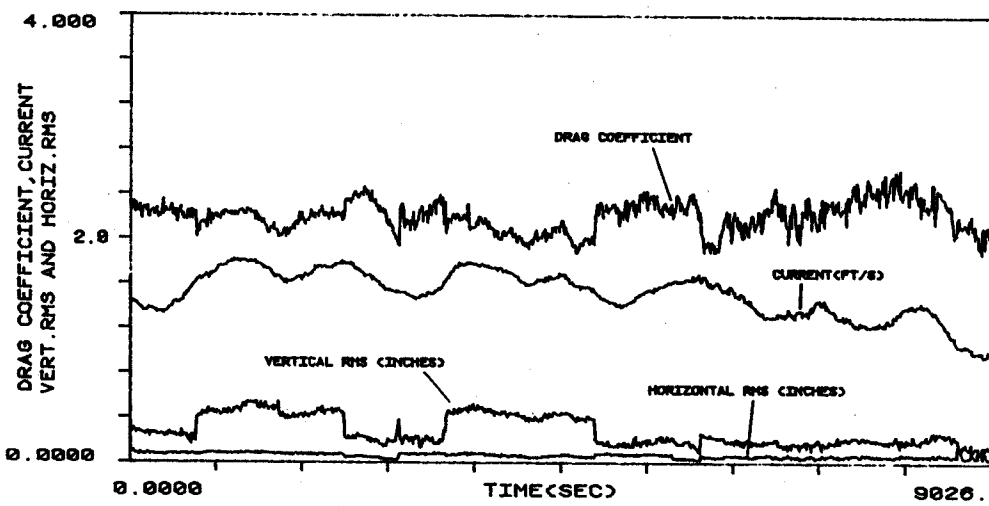


Fig. 6—Drag coefficient, current, and RMS displacement at 2L/5 for the cable with stranded plastic.

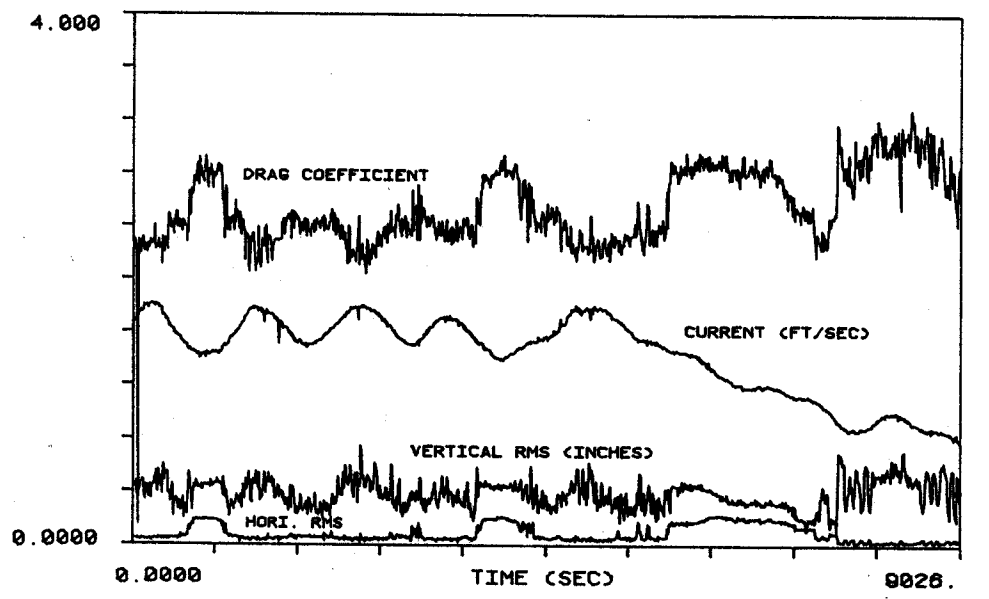


Fig. 7—Drag coefficient, current, and RMS displacement at 3L/4 for the cable with six lumps.

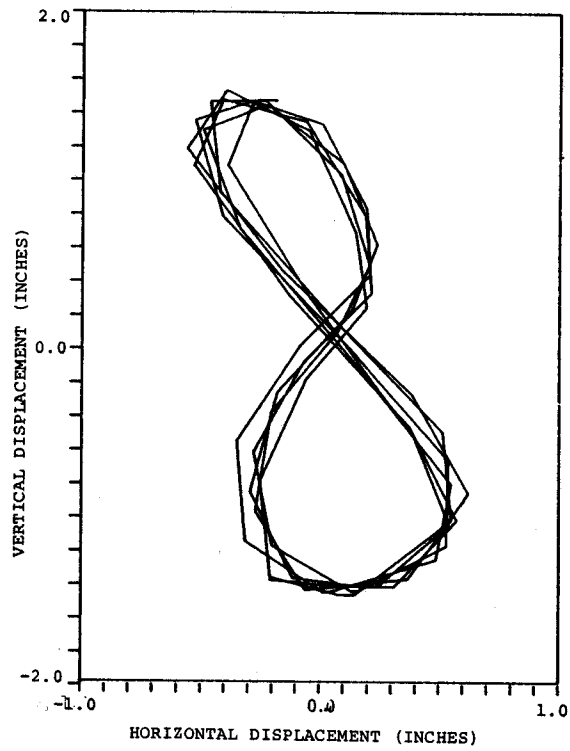


Fig. 8—Pipe lock-in response at L/2.

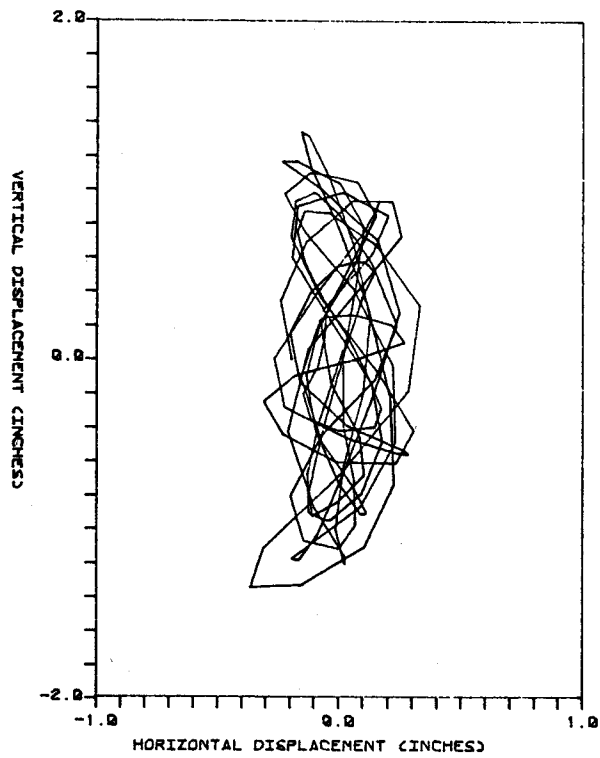


Fig. 9—Pipe nonlock-in response at L/8.

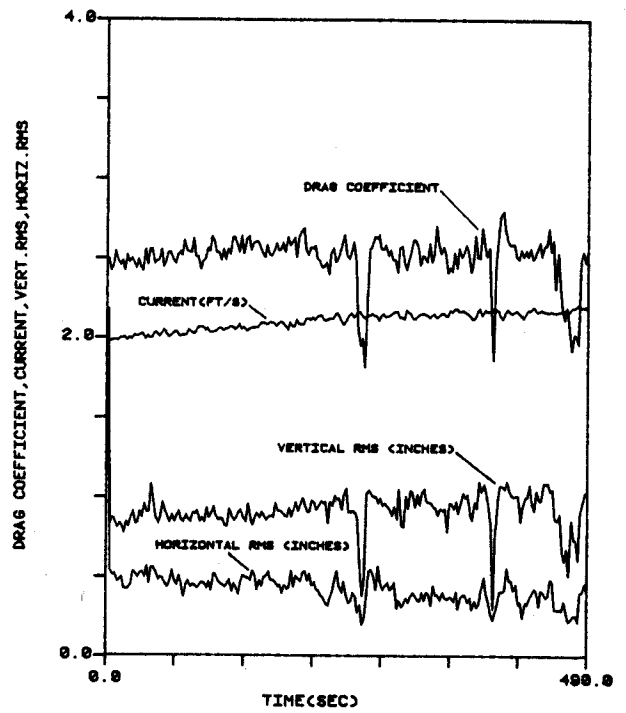


Fig. 10—Pipe drag coefficient and displacement at L/6. Third mode cross flow and fifth mode in-line response.